Mathematical Biosciences and Engineering

http://www.aimspress.com/journal/MBE

MBE, 23(5): 1340–1355.
DOI: 10.3934/mbe.2026049
Received: 10 February 2026
Revised: 16 March 2026
Accepted: 20 March 2026
Published: 02 April 2026

Research article

Oscillations in marine and insect populations with delayed density-dependence

Thomas Erneux[1,*] **and Yang Kuang**[2,†]

[1] Physique des Systèmes Dynamiques, Université Libre de Bruxelles, Campus Plaine, C.P. 231, 1050 Bruxelles, Belgium

[2] School of Mathematical and Statistical Sciences, Arizona State University, Tempe, AZ 85287, USA

* **Correspondence:** Email: thomas.erneux@ulb.be.

Abstract: A scalar delay differential equation with threshold nonlinearity has been formulated to describe the limited growth of sessile marine invertebrates and insect populations when resources are limited. Depending on the settlement and mortality rates of juveniles, sustained oscillations generated by Hopf bifurcations are possible. We construct these time-periodic solutions by using the method of steps and analyze their bifurcation properties. All our analytical results are in agreement with those obtained from numerical simulations of the original delay differential equation. Particular attention is devoted to the Hopf bifurcation points in the limit of a high juvenile settlement rate. In addition, we identify important changes in the periodic waveform when adults exhibit low mortality rates.

Keywords: oscillation; periodic solution; delay differential equation; marine population model; density-dependence

1. Introduction

Delayed density-dependence has been used by ecologists to explain population cycles [1, 2]. Populations are allowed to increase above their normal capacity because there is a time lag until a negative feedback mechanism brings the population back down [3]. The causes of a delayed density-dependence vary among species and range from food supply and predation to competition between life stages. This is the case of corals, which have a life history with two distinct phases: the larval phase, where the coral is motile, and the sessile phase, where the coral is cemented to a substrate and unable to move on its own. Coral larvae, known as recruits, settle onto unoccupied areas of the reef and begin to spread out to form colonies. As larvae rarely settle on living colonies, recruitment depends on coral coverage and is proportional to the amount of free space available in the reef. The amount of free space available to settle can be severely limiting and thus may act as a form of density-dependence. This density-dependence

[†] In memory of Stephen Gourley who was our friend, colleague, and a gifted teacher.

has led to the view that space-limited recruitment represents a regulating physical mechanism. In order to better understand these processes, Roughgarden et al. [4] proposed an age-structured demographic model suitable for open marine populations. Although intended for barnacle populations, the model is equally relevant for many single species populations of sessile marine invertebrates that have a pelagic larval phase [5].

Later, Bence and Nisbet [6] revisited the hypotheses of Roughgarden et al. hypothesizes and emphasized the destabilizing role of a time delay when older or larger individuals may inhibit the recruitment of juveniles. Bence and Nisbet were motivated by the biology of the California giant kelp. Giant kelp is a major structure-forming marine plant on hard substrates in the shallow subtidal habitat along the California coast [7]. Shading by the largest plants reduces the rate of recruitment of the youngest stages. However, some finite time is required before the young plants grow sufficiently to contribute to shading. Bence and Nisbet [6] analyzed the following delay differential equation (DDE) for the adult population N:

$$\frac{dN}{dt} = \exp(-m_J\tau)F(t-\tau) - mN, \tag{1.1}$$

where

$$F(t) \equiv r\,[1 - aN(t)]_+ = \left[\begin{array}{c} r(1-aN(t)) \text{ if } aN(t) < 1, \\ 0 \text{ otherwise} \end{array}\right]. \tag{1.2}$$

The function (1.2) represents the proportion of space that is available, and $a > 0$ is the amount of space occupied by an individual adult. In this model each individual takes up an equal amount of space until all space has been occupied. The expression (1.2) prevents $F(t)$ from becoming negative when there are more than enough individuals to fill all the space. There is a fixed time delay τ between settlement and recruitment into the adult population. The parameter r is the settlement rate of the juveniles, and $\exp(-m_J\tau)$ is the through-stage survival probability of juveniles. The parameters m_J and m denote the mortality rates for juveniles and adults, respectively. The derivation of these equations from an age-structured population model [8,9] that takes into account space limitation was originally proposed by Roughgarden et al. [4] and was later supplemented by the maturation delay [6]. Appendix A reviews the derivation from the original age-structured model emphasizing the simplifying hypothesizes needed for the formulation of Eq (1.1). Note from the expression of (1.2) that the juveniles are assumed to occupy no space. Their effect is implicit through the exponential term $\exp(-m_J\tau)$. Models where juveniles may occupy some space were formulated in References [6] and [10] but their equations lost the simplicity of Eq (1.1).

Britton [11] (p25, Eq 1.7.17) considered Eq (1.1) with $m_J = 0$ for insect populations limited by their resources. The motivation came from Nicholson laboratory experiments showing that population of blowflies oscillates in amplitude when resources for the adults are limited. $N(t)$ denotes the number of adult insects at time t. The function $F(t)$ represents the excess rate of food supply where τ is the time it takes for an egg to become an adult.

By contrast to ordinary differential equations, the study of delay differential equations (DDEs) is harder because of their infinite-dimensional nature: the solution of a DDE depends on the function's history, not just its current state, requiring an initial function over a time interval to define a unique trajectory. Scalar DDEs exhibiting piecewise linear or piecewise constants as nonlinearities have proven to be useful when we are modeling biological control mechanisms. Periodic solutions may be computed explicitly allowing the determination of extrema and period. This is typically the case for physiological

control problems involving a strong negative feedback. A negative feedback slows or stops a reaction. It may involve a time delay, which is needed for signal transduction and transcription, translation, and the formation of biochemical species [12, 13]. If the delay is too large, however, the control loop looses its landmarks (it doesn't remember its state so long ago) and exhibits oscillations. The Mackey equation [14, 15]

$$\frac{dy}{dt} = \frac{1}{1 + y^n(t-\tau)} - by \tag{1.3}$$

is a popular DDE that has been considered for different purposes [16–18]. The nonlinear function in Eq (1.3) is a Hill function that is based on the law of mass action for the binding of molecules [19]. Equation (1.3) has been the source of many numerical and analytical studies [16, 19]. In the strong feedback limit ($n \to \infty$), Eq (1.3) approaches the DDE

$$\frac{dy}{dt} = -by + \left[\begin{array}{l} 0 \text{ if } y(t-\tau) > 1 \\ 1 \text{ if } y(t-\tau) < 1 \end{array} \right], \tag{1.4}$$

exhibiting piecewise constants as nonlinearity. Eq (1.4) admits stable time periodic solutions if $0 < b < 1$. They have been constructed analytically by using the method of steps [20].

In the context of growing populations limited by space, we consider Eq (1.1) as a basic mathematical model when older or larger individuals inhibit the recruitment of juveniles. A graphical study of the linear stability properties of the steady state, as well as numerical simulations of periodic oscillations, have been presented in [6], and a global qualitative analysis of Eq (1.1) can be found in [10]. As for Eq (1.4), we propose to solve this equation by the method of steps which now depends on piecewise linear functions of the dependent variable rather than piecewise constants. Section 2 concentrates on the linear stability analysis of the steady state and determines a domain of unstable states in the r versus τ parameter space. A branch of stable periodic solutions are delimited by two successive Hopf bifurcations. The construction of a periodic solution between these Hopf bifurcations makes it necessary to solve Eq (1.1) in specific intervals of time marked by the change of sign of $aN(t-\tau) - 1$. Details of the analysis are relegated in Appendix B for mathematical clarity. In Section 3, we describe the extrema of the periodic solutions as functions of τ. In Section 4, we discuss the dependence of the two dimensionless parameters with respect to the delay and to the change of the oscillatory wave form as the mortality rate of the adults decreases.

2. Steady state and Hopf bifurcations

In this section, we summarize the results of a linear stability analysis. The steady state solution of Eq (1.1) is given by

$$N_s = \frac{r \exp(-m_J \tau)}{m + ra \exp(-m_J \tau)} \tag{2.1}$$

and is a monotone function of r with $N_s(0) = 0$ and $N_s(\infty) = 1/a$. From the linearized equation, we determine the characteristic equation for the growth rate λ given by

$$\lambda + \exp(-m_J \tau) ra \exp(-\lambda \tau) + m = 0. \tag{2.2}$$

By inserting $\lambda = i\omega$ into Eq (2.2), we obtain the Hopf bifurcation conditions from the real and imaginary parts:

$$\exp(-m_J \tau) ra \cos(\omega \tau) + m = 0, \tag{2.3}$$

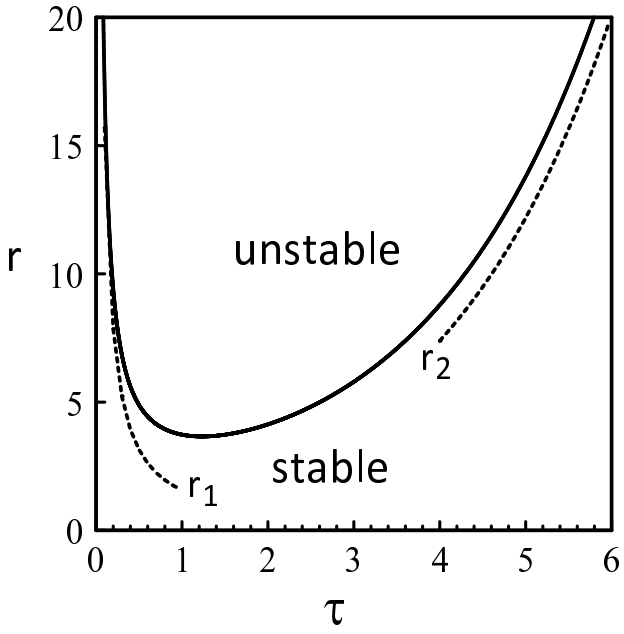

Figure 1. The Hopf bifurcation line in the (τ, r) parameter space. It is obtained from Eqs (2.5) and (2.6) by progressively increasing y from $\pi/2$ to π. At a fixed value of r, the domain of unstable steady states is delimited by two Hopf bifurcation points. The values of the fixed parameters are $a = m = 1$ and $m_J = 0.5$. The broken lines r_1 and r_2 are the approximations (2.7) and (2.8) for $\tau \to 0$ and $\tau \to \infty$, respectively. Recall that the Hopf bifurcation point for the delayed logistic equation $N' = kN(1 - N(t - \tau))$ is $k = \pi/(2\tau)$ [1, 20] which is identical to (2.7) ($k = ar$). Equation (1.1), however, admits another Hopf bifurcation for larger values of τ emphasizing the role of the delay induced death rate $\exp(-m_J\tau)$.

$$\omega - \exp(-m_J\tau) ra \sin(\omega\tau) \quad = \quad 0. \tag{2.4}$$

We wish to find the first Hopf bifurcation in terms of r and τ. It marks the change of stability of the steady state. An elegant representation of its solution is obtained in parametric form. $y \equiv \omega\tau$ is the parameter and represents the dimensionless Hopf bifurcation frequency (ω normalized by $1/\tau$). It is obtained by eliminating $\exp(-m_J\tau)$ in Eq (2.3) using Eq (2.4). It leads to a single equation for $\tau = \tau(y)$. Having τ, we obtain $r = r(y)$ from Eq (2.3). The expressions of $\tau = \tau(y)$ and $r = r(y)$ are

$$\tau \quad = \quad -\frac{y}{m \tan(y)}, \tag{2.5}$$

$$r \quad = \quad -\frac{m \exp(m_J\tau)}{a \cos(y)}. \tag{2.6}$$

The Hopf bifurcation line in the (τ, r) parameter space is shown in Figure 1. It has been obtained from Eqs (2.5) and (2.6) by progressively changing y from $\pi/2$ to π. For large values of r, the left and right branches of the Hopf bifurcation line admit simple limits. Inserting $y = \pi/2 + u$ ($u > 0$) into Eqs (2.5) and (2.6), we find $\tau \to \pi u/(2m)$ and $r \to m/(au)$ as $u \to 0^+$. Eliminating u we obtain the approximation

$$r_1 = \frac{\pi}{2a\tau} \ (\tau \to 0). \tag{2.7}$$

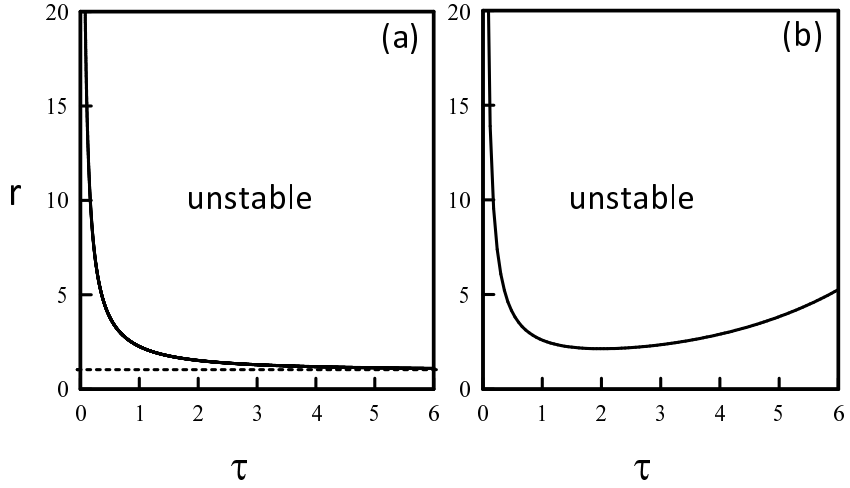

Figure 2. Hopf bifurcation curves in the r vs τ parameter space. They have been obtained from Eqs (2.5) and (2.6). The parameters have the same values as in Figure 1 except (a) $m_J \to 0$ and (b) $m \to 0$.

Similarly, inserting $y = \pi + v$ ($v < 0$) into Eqs (2.5) and (2.6), we find $\tau \to -\pi/(mv)$ and $r \to m\exp(m_j\tau)/a$ as $v \to 0^-$. The second limit gives $r = r(\tau)$ as

$$r_2 = \frac{m}{a}\exp(m_J\tau)\ (\tau \to \infty). \tag{2.8}$$

The expressions (2.7) and (2.8) are the leading asymptotic approximations of the Hopf bifurcation line as $\tau \to 0$ and $\tau \to \infty$, respectively. They are shown by broken lines in Figure 1. The expressions for the correction u and v for $y \equiv \omega\tau$ will be useful when we analyze the period of the oscillations near the two Hopf bifurcation points (see Section 3.2). They are given by

$$u = \frac{m}{ar} \text{ and } v = -\frac{\pi m_J}{m\ln(ar/m)}. \tag{2.9}$$

We note from (2.7) and (2.8) that the mortality rate of the juveniles m_J only affects r_2. As $m_J \to 0$, r_2 approaches the constant value m/a, consistent with the analysis of Britton [11], who studied the case $m_J = 0$. See Figure 2(a). On the other hand, a non-zero m_J has a stabilizing effect since r_2 moves to the left as we increase m_J while r_1 remains unchanged.

Another interesting case appears when the mortality rates for the adults m is low. Introducing $y = \pi/2 + w$ into Eqs (2.5) and (2.6), assuming $w = O(m)$ and $r = O(m)$, we obtain $\tau \to -\pi w/(2m)$ and $r \to -m\exp(m_J\tau)/(aw)$. Eliminating m in both expressions, we find an equation for $r = r(\tau)$ given by

$$r = \frac{\pi}{2a\tau}\exp(m_J\tau). \tag{2.10}$$

The function (2.10) is shown in Figure 2(b). As $\tau \to 0$, we note from (2.10) that $r \to \infty$ as $r = r_1$, given by Eq (2.7). As we increase τ from zero, (2.10) has a minimum at $\tau_{\min} = 1/m_J$ and then grows exponentially. Note that the strict values $m_J = 0$ and $m = 0$ are not biological since they represent mortality rates.

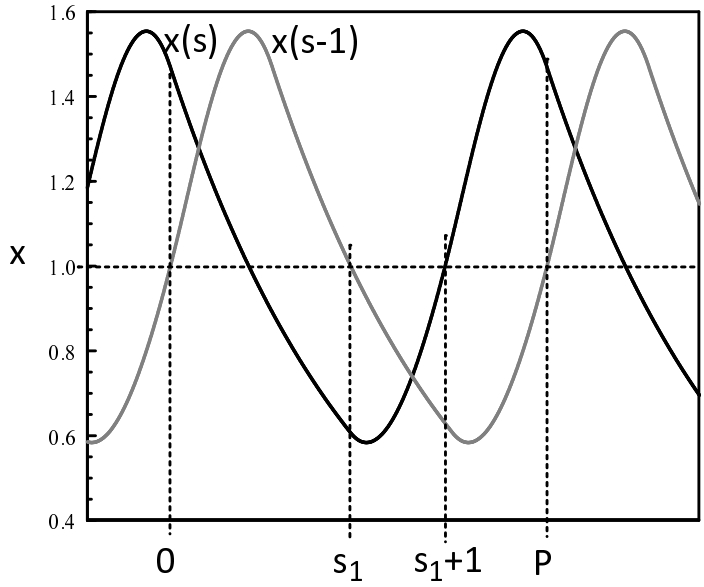

Figure 3. Periodic solution of Eq (B.2). The fixed original parameters are $a = m = 1$, $m_J = 0.5$, $r = 10$, $\tau = 0.5$. The dimensionless parameters are $b \equiv ra\tau \exp(-m_J\tau) = 3.894$ and $c \equiv m\tau = 0.5$. The vertical dotted lines mark the points where $1 - x(s-1)$ is zero: $s_0 = 0$, $s_1 \simeq 1.76$, $s_1 + 1 = 2.76$, and $P = 3.7$. The corresponding values of x are: $x(0) = x_0 \simeq 1.47$, $x(s_1) = x_1 \simeq 0.61$, $x(s_{1+1}) = x_2 \simeq 1.07$, and $x(P) = x_0$.

3. Limit-cycle oscillations

A typical time periodic solution in terms of the dimensionless variables $x = aN$ and $s \equiv t/\tau$ is shown in Figure 3. It has been obtained by integrating Eq (B.2), and both $x(s)$ and $x(s-1)$ are shown in the figure. The evolution of $x(s)$ during one period shows three distinct parts, namely (1) $0 \le s \le s_1$, (2) $s_1 \le s \le s_1 + 1$, and (3) $s_1 + 1 \le s \le P$. For each part, the function $1 - x(s-1)$ in Eq (B.2) takes different expressions of s, allowing us to solve ordinary differential equations step by step. In the following analysis, we assume that

$$s_1 > 1 > s_p - s_1 - 1, \tag{3.1}$$

which applies for a large range of values of τ. If one of these inequalities is not verified, we need to proceed with a different division scheme.

In Appendix B, Eqs (1.1) and (1.2) are formulated in the dimensionless equation (B.2), which is then solved step by step. In this section, we concentrate on the extrema of the oscillations as functions of τ and analyze the Hopf bifurcation transitions.

3.1. Extrema

From (B.11), we determine the time of the minimum of x by using the condition $dx/ds = 0$. We obtain

$$s_{\min} - s_1 = \frac{\exp(-c)}{b}. \tag{3.2}$$

Inserting (3.2) into (B.11), we find

$$x_{\min} = \frac{b}{c}\left[1 - \exp\left(-\frac{c}{b}\exp(-c)\right)\right]. \tag{3.3}$$

The time of the maximum of x is obtained from (B.16) by using the condition $dx/ds = 0$. We find that the time interval $u_{\max} \equiv s_{\max} - s_1 - 1$ satisfies the following quadratic equation:

$$-\exp(-c)(\exp(-c) - b) + b\exp(-c)u_{\max} - \frac{b^2}{2}u_{\max}^2 = 0. \tag{3.4}$$

The maximum $x_{\max}$ is then obtained by evaluating (B.16) at $s = s_{\max}$:

$$\begin{aligned} x_{\max} \;=\; & \left[\exp(-c)(\exp(-c) - \frac{b}{c} - b) + (\frac{b}{c})^2\right]\exp(-cu_{\max}) \\ & + \frac{b}{c}(1 - \frac{b}{c}) \\ & - \left[\exp(-c) - \frac{b}{c}\right] bu_{\max}\exp(-cu_{\max}) \\ & + \frac{b^2}{2}u_{\max}^2\exp(-cu_{\max}). \end{aligned} \tag{3.5}$$

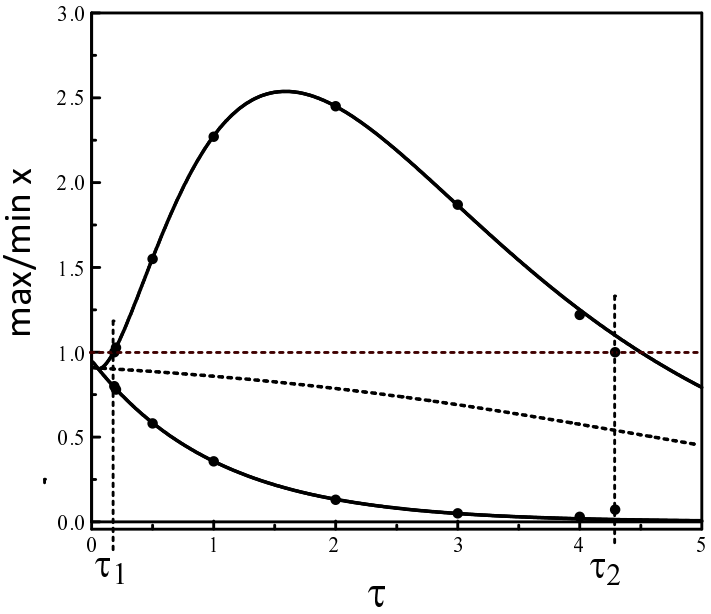

Figure 4. Analytical vs numerical bifurcation diagrams. $r = 10$, $a = m = 1$, and $m_j = 0.5$. The broken line is the steady state solution $x = b/(b + c)$. The dotted lines are the extrema of the periodic solutions given by (3.3) and (3.5). Dots are extrema obtained numerically from integrating Eq (B.2). The lower and upper Hopf bifurcation points are located at $\tau_1 = 0.185$ and $\tau_2 = 4.292$, respectively. We observe that the amplitude of the oscillations decreases for large time delays until stability is recovered. It suggests that longer maturation delays moderate the size of the oscillations before full stability is reached.

Figure 4 compares the extrema of $x(t)$ given by (3.3) and (3.5) with their numerical estimates obtained from simulating Eq (B.2). The agreement is excellent except near the Hopf bifurcation points. Near these points, the condition (3.1) is no longer verified because $t_1 - t_0 << 1$.

3.2. Hopf bifurcations

At the Hopf bifurcation points, the periodic solution verifies a linear first order DDE and is harmonic in time. The amplitude of the oscillations is arbitrary provided the maxima verifies the inequality $\max(x) \leq 1$. As we come close to the Hopf bifurcation points (specifically, as $\tau - \tau_1 \to 0^+$ or $\tau - \tau_2 \to 0^-$), the periodic solution approaches

$$x = x_s(\tau_j) + (1 - x_s(\tau_j))\cos(y_j s) \quad (j = 1, 2), \tag{3.6}$$

where x_s is the steady state, and y_j is the dimensionless frequency $y \equiv \omega\tau$ evaluated at the Hopf bifurcation point. See Figure 5. We note that during a very short time interval, $x(s) > 1$, which is enough to sustain a stable time-periodic solution. The period of the oscillations determined numerically are (a) $P_1 = 3.75$ and (b) $P_2 = 2.43$, implying $y_1(num) = 1.68$ and $y_2(num) = 2.79$, respectively. With $y_1 = \pi/2 + u$ and $y_2 = \pi + v$, where u and v are given by (2.9), we determine analytical estimates of the frequencies:

$$y_1(anal) = \omega\tau_1 = \frac{\pi}{2} + \frac{m}{ar} = 1.67, \tag{3.7}$$

$$y_2(anal) = \omega\tau_2 = \pi - \frac{\pi m_J}{m\ln(ar/m)} = 2.46. \tag{3.8}$$

$y_1(anal)$ agrees with the numerical estimate $y_1(num)$ while $y_2(anal)$ exhibits a 12% difference from $y_2(num)$. Their leading approximations $y_1 = \pi/2$ and $y_2 = \pi$ emphasize different periods ($P = 4$ and 2, respectively) as the branch of periodic solutions starts and ends at the two Hopf bifurcation points.

4. Discussion

Equations (1.1) and (1.2) represent a drastic simplification of the evolution equations for a biological population but allow us to identify key physical mechanisms causing cyclic fluctuations. In dimensionless form, our dynamical problem is described by Eq (B.2), which exhibits two parameters, namely $b = ra\tau\exp(-m_J\tau)$, the settlement rate of the juveniles limited by their survival probability, and $c = m\tau$, the mortality rate of the adults. If the time delay τ is clearly responsible for the oscillatory instability, it acts differently on b and c. As τ increases from zero, c increases linearly with τ while b first increases, reaches a maximum at $\tau = 1/m_J$, and then decays exponentially to zero. This dependence of b with respect to τ explains why the settlement rate of the juveniles r needs to be sufficiently large to observe an instability at a low value of the delay and why the basic steady state recovers its stability at large values of τ.

The construction of the time periodic solution by the method of successive steps led to analytical expressions of their extrema, shown in the bifurcation diagram (Figure 4). The steady state looses its stability at a low value of τ through a Hopf bifurcation. The amplitudes of the oscillations at that point are small, increase with τ, reach a maximum close to the maximum value of b ($\tau = 1/m_J = 2$), and disappear at the second Hopf bifurcation where the minima of the oscillations are close to zero. The periods of the oscillations progressively decrease from 4 to 2 between the two bifurcation points.

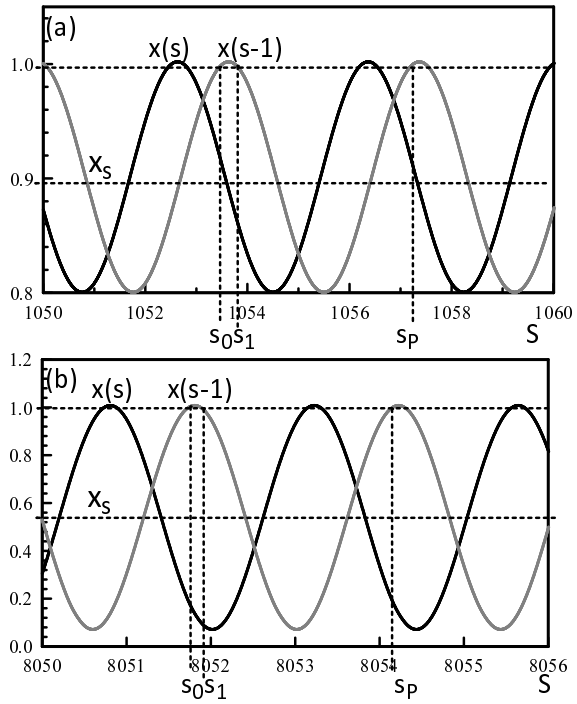

Figure 5. Periodic solutions obtained numerically from Eq (B.2). Black and grey lines correspond to $x(s)$ and $x(s-1)$. The same values from Figure 1 are used for the fixed parameters and $r = 10$. (a) $\tau = 0.1860 > \tau_1 = 0.1856$; (b) $\tau = 4.2900 < \tau_2 = 4.2918$. s_0 and s_1 delimit the short interval of time where $x(s-1) > 1$. The interval $s_P - s_0$ represents the period.

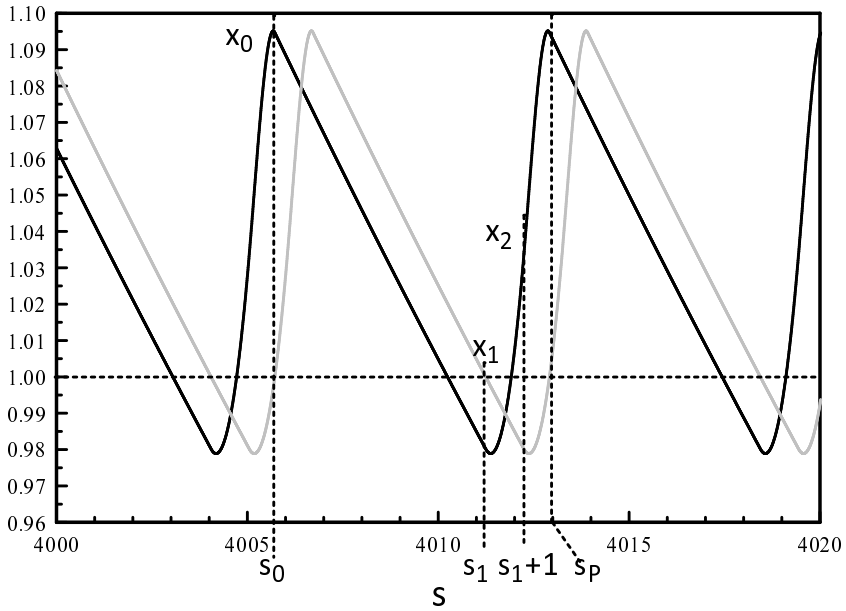

Figure 6. Sustained oscillations for small values of m. The parameters are: $r = 10$, $\tau = 2$, $a = 1$, $m_J = 0.5$, and $m = 10^{-2}$. The different points in the figure are $x_0 = 1.0946$ at $s_0 = 4005.71$, $x_1 = 0.9803$ at $s_1 = 4011.24$, and $x_2 = 1.0332$ at $s_1 + 1$. We have verified that they match the analytical predictions derived in Appendix B.

The wave forms of the periodic solutions change from nearly sinusoidal to sawtooth if $c < 1$, indicating a low mortality rate for the adults. Figure 6 shows a typical example where a slow decay of x is followed by a relatively fast increase of x. The slow decrease of the adult population clearly dominates the oscillatory evolution. What is not so obvious is the small amplitude oscillations near $x = 1$. This results from the fact that the threshold amplitude for generating a pulsating response ($x = 1$) is slightly above its steady state value ($x_s = 1 - cb + O(c^2)$).

We conclude with a remark on the utility of simple DDE models in biology already addressed in the introduction. The piecewise linear DDE model explored in this paper clearly helped Bence and Nisbet [6] to understand the hypotheses of Roughgarden et al. [4]. Mathematically, it allowed an analysis of the bifurcation diagram, in terms of the parameters, as an alternative to numerical simulations.

Use of AI tools declaration

The authors declare they have not used artificial intelligence (AI) tools in the creation of this article.

Acknowledgments

On June 25–29, 2007, a minicourse on delay differential equations was organized at the University of Utah. Lectures were shared by the two authors and by Stephen Gourley. TE acknowledges the impact of his collegues on problems in population dynamics. Y.K. is supported by the U.S. NSF grant DMS-2325146, DMS-2421258, and NIH grant 1R01AI192873-01.

Conflict of interest

The authors have no conflicts of interest to declare. Yang Kuang is an editor-in-chief for Mathematical Biosciences and Engineering and was not involved in the editorial review or the decision to publish this article.

References

1. Y. Kuang, *Delay Diffferential Equations: With Applications in Population Dynamics*, Academic Press, 1993.
2. H. Wang, J. D. Nagy, O. Gilg, Y. Kuang, The roles of predator maturation delay and functional response in determining the periodicity of predator–prey cycles, *Math. Biosci.*, **221** (2009), 1–10. https://doi.org/10.1016/j.mbs.2009.06.004
3. S. A. Gourley, Y. Kuang, A stage structured predator-prey model and its dependence on maturation delay and death rate, *J. Math. Biol.*, **49** (2004), 188–200.
4. J. Roughgarden, Y. Iwasa, C. Baxter, Demographic theory for an open marine population with space-limited recruitment, *Ecology*, **66** (1985), 54–67. https://doi.org/10.2307/1941306
5. Y. Artzy-Randrup, R. Olinky, L. Stone, Size-structured demographic models of coral populations, *J. Theor. Biol.*, **245** (2007), 482–497. https://doi.org/10.1016/j.jtbi.2006.10.019
6. J. R. Bence, R. M. Nisbet, Space-limited recruitment in open systems: The importance of time delays, *Ecology*, **70** (1989), 1434–1441. https://doi.org/10.2307/1938202

7. R. M. Nisbet, J. R. Bence, Alternative dynamic regimes for canopy-forming kelp: A variant on density-vague population regulation, *Am. Nat.*, **134** (1989), 377–408. https://doi.org/10.1086/284987
8. R. E. Baker, *Further Mathematical Biology Lecture Notes*, University of Oxford, 2021.
9. S. L. Robertson, S. M. Henson, T. Robertson, J. M. Cushing, A matter of maturity: To delay or not to delay? Continuous-time compartmental models of structured populations in the literature 2000–2016, *Nat. Resource Mod.*, **31** (2018), e12160.
10. Y. Kuang, J. W. H. So, Analysis of a delayed two-stage population model with space-limited recruitment, *SIAM J. Appl. Math.*, **55** (1995), 1675–1696. https://doi.org/10.1137/S0036139993252839
11. N. F. Britton, *Essential Mathematical Biolgy*, Springer Undergraduate Mathematics Series, Springer-Verlag, London, 2003.
12. A. B. Börsch, J. Schaber, How time delay and network design shape response patterns in biochemical negative feedback systems, *BMC Syst. Biol.*, **10** (2016), 82.
13. A. Hoffmann, A. Levchenko, M. L. Scott, D. Baltimore, The IkB-NF-kB signaling module: Temporal control and selective gene activation, *Science*, **298** (2002), 1241–1245. https://doi.org/10.1126/science.1071914
14. M. C. Mackey, L. Glass, Oscillation and chaos in physiological control systems, *Science*, **197** (1977), 287–289. https://doi.org/10.1126/science.267326
15. M. C. Mackey, Mathematical models of hematopoietic cell replication and control, in *The Art of Mathematical Modelling: Case Studies in Ecology, Physiology and Biofluids* (eds. H. G. Othmer, F. R. Adler, M. A. Lewis, and J. C. Dallon), Prentice Hall, New Jersey, (1997), 149–178.
16. C. P. Fall, E. S. Marland, J. M. Wagner, J. J. Tyson, *Computational Cell Biology*, Springer, New York, 2022.
17. A. Beuter, L. Glass, M. C. Mackey, M. Titcombe, *Nonlinear Dynamics in Physiology and Medicine*, Springer, New York, 2003.
18. J. Milton, T. Ohira, *Mathematics as a Laboratory Tool*, Springer, New York, 2014. https://doi.org/10.1007/978-1-4614-9096-8
19. J. Milton, Pupil light reflex: Delays and oscillations, in *Nonlinear Dynamics in Physiology and Medicine*, Springer, New York, (2003), 271–301.
20. T. Erneux, *Applied Delay Diffferential Equations*, Springer, 2009. https://doi.org/10.1007/978-0-387-74372-1_8
21. E. Liz, E. Trofimchuk, S. Trofimchuk, Mackey–Glass type delay differential equations near the boundary of absolute stability, *J. Math. Anal. Appl.*, **275** (2002), 747–760. https://doi.org/10.1016/S0022-247X(02)00416-X
22. A. Ivanov, S. Shelyag, Explicit periodic solutions in a delay differential equation, in *Addressing Modern Challenges in the Mathematical, Statistical, and Computational Sciences* (eds. D. M. Kilgour, H. Kunze, R. N. Makarov, R. Melnik, X. Wang), Springer Nature Switzerland, (2023), 459–466.

Appendix

A. Age structure

The purpose of this appendix is to derive Eqs (1.1) and (1.2) from an age-structured model. It requires simple assumptions on the death rates of juveniles and adults as well as the fact that juveniles occupy no space before becoming adults.

Roughgarden et al. [4] formulated an age-structured model for the population density of age x at time t, denoted by $n(x, t)$. It satisfies the transport equation

$$n_t + n_x = -d(x)n, \tag{A.1}$$

where $d(x)$ is the mortality function. Equation (A.1) is to be solved with the initial condition at $t = 0$,

$$n(x, 0) = n_0(x) = 0, \tag{A.2}$$

which is assumed to be zero. [4]. Let $F(t)$ be the free space at time t, s the instantaneous settling rate per unit of free space, and $a(x)$ the size of an individual of age x. Then, the birth of new organisms entering at age zero is given by

$$n(0, t) = sF(t) = s\left[1 - \int_0^\infty a(x)n(x, t)dx\right]_+ . \tag{A.3}$$

In the expression of $F(t)$, the number 1 represents the normalized total area of available substrate while the integral is the occupied space by the individuals at time t.

Equation (A.1) describes the evolution of individuals that have settled into the system. Equation (A.2) relates the number of newly settled individuals to the amount of free space, and condition (A.3) is equivalent to the conservation of total space. $[y]_+ = y$ if $y \geq 0$ and $[y]_+ = 0$ if $y < 0$. The latter prevents the free space $F(t)$ from becoming negative. Equation (A.1) is to be solved in the positive quadrant of the (t, x) plane with the conditions (A.2) and (A.3). We may think of travelling in this plane along a line that we determine by applying the method of characteristics [11]. Specifically, we find that

$$n(x, t) = \left\{ \begin{array}{c} sF(t - x)\exp(-\int_0^x d(y)dy), \quad 0 < x < t, \\ 0, \quad 0 < t < x \end{array} \right\}. \tag{A.4}$$

Let $\tau > 0$ be the maturation age of the juveniles. We assume that the death rates for juveniles and adults are d_J and d_A, respectively:

$$d(x) = \left[\begin{array}{c} d_J \text{ for } 0 \leq x < \tau \\ d_A \text{ for } \tau \leq x \end{array} \right]. \tag{A.5}$$

The numbers of juveniles $J(t)$ and adults $A(t)$ are given by the integrals

$$J(t) \equiv \int_0^\tau n(x, t)dx \text{ and } A(t) \equiv \int_\tau^\infty n(x, t)dx, \tag{A.6}$$

respectively.

For $x \leq \tau \leq t$, the solution (A.4) using (A.5) becomes

$$n(x,t) = sF(t-x)\exp(-d_J x). \tag{A.7}$$

which allows us to determine $n(x,t)$ at $x = \tau$:

$$n(\tau,t) = sF(t-\tau)\exp(-d_J\tau) \ \ (t \geq \tau). \tag{A.8}$$

Integration of (A.1) with respect to x over the juvenile stage ($x = 0$ to $x = \tau$) yields

$$\frac{dJ}{dt} + n(\tau,t) - n(0,t) = -d_J J. \tag{A.9}$$

Inserting (A.8) into Eq (A.9) and using (A.4) for $n(0,t)$, we obtain ($t \geq \tau$)

$$\frac{dJ}{dt} = -sF(t-\tau)\exp(-d_J\tau) + sF(t) - d_J J. \tag{A.10}$$

On the other hand, integration of (A.1) with respect to x over the adult stage ($x = \tau$ to $x = \infty$) yields (assuming $n(\infty,t) = 0$)

$$\frac{dA}{dt} + 0 - n(\tau,t) = -d_A A \tag{A.11}$$

from which we obtain ($t \geq \tau$)

$$\frac{dA}{dt} = sF(t-\tau)\exp(-d_J\tau) - d_A A. \tag{A.12}$$

Equations (A.10) and (A.12) are two DDEs for J and A valid for $t \geq \tau$. The juveniles are assumed to occupy no space. By assuming

$$a(x) = \left\{ \begin{array}{c} a_A \text{ if } x > \tau \\ 0 \text{ if } x \leq \tau \end{array} \right\}, \tag{A.13}$$

$F(t)$ simplifies as

$$F(t) = \left[1 - a_A \int_\tau^\infty n(x,t)dx\right]_+ = \left[1 - a_A A(t)\right]_+ . \tag{A.14}$$

Inserting (A.14) into Eqs (A.10) and (A.12) leads to two linear DDEs for J and A given by

$$\frac{dJ}{dt} = s\left[1 - a_A A(t-\tau)\right]_+ \exp(-d_J\tau) + s\left[1 - A\right]_+ - d_J J, \tag{A.15}$$

$$\frac{dA}{dt} = s\left[1 - a_A A(t-\tau)\right]_+ \exp(-d_J\tau) - d_A A. \tag{A.16}$$

The transition rate between the juvenile and adult classes has a time delay τ, which is the age of maturation. The delay τ appears in both differential equations. Note however that the A equation is uncoupled from the J equation. Eq (A.16) is Eq (1.1) with N, a, m_J, and m replacing A, a_A, d_J, and d_A, respectively.

B. Periodic solutions

By introducing the new variables

$$x \equiv aN \text{ and } s \equiv t/\tau \tag{B.1}$$

into Eq (1.1), we determine

$$\frac{dx}{ds} = b\,[1 - x(s-1)]_+ - cx, \tag{B.2}$$

where

$$b \equiv ra\tau \exp(-m_J\tau) \text{ and } c \equiv m\tau. \tag{B.3}$$

The DDE (B.2) now depends on only two dimensionless parameters. Recall that $[y]_+ = y$ if $y < 1$, and 0 otherwise. A typical time-periodic solution of Eq (B.2) has been determined numerically and is shown in Figure 3. During one period, the solution consists of three parts where Eq (B.2) takes different forms. We analyze each part sequentially.

B.1. $0 \le s \le s_1$

We first consider the time interval $0 \le s \le s_1$ where $x(s-1) \ge 1$. Equation (B.2) then reduces to

$$\frac{dx}{ds} = -cx,\ x(0) = x_0, \tag{B.4}$$

where x_0 is unknown. Equation (B.4) means that the adult population is naturally decaying without any effects of the juveniles. Equation (B.4) has the solution

$$x(s) = x_0 \exp(-cs). \tag{B.5}$$

At time $s = s_1$, $x(s)$ takes the value

$$x(s_1) = x_1 \equiv x_0 \exp(-cs_1). \tag{B.6}$$

But because $x(s_1 - 1) = 1$, we find from (B.5), evaluated at $s = s_1 - 1$, the condition

$$x(s_1 - 1) = x_0 \exp(-c(s_1 - 1)) = 1. \tag{B.7}$$

Using (B.7), we may simplify (B.6) and find x_1 as

$$\underline{x_1 = \exp(-c).} \tag{B.8}$$

B.2. $s_1 \le s \le s_1 + 1$

We next consider the time interval $s_1 \le s \le s_1 + 1$ where $x(s-1) \le 1$. During this interval, we note from Figure 3 that

$$x(s-1) = \exp(-c(s - s_1)). \tag{B.9}$$

Equation (B.2) now becomes

$$\frac{dx}{ds} = b\,[1 - \exp(-c(s - s_1))] - cx,\ x(s_1) = x_1. \tag{B.10}$$

The current growth of the adult population depends on its evolution in the past. Equation (B.10) admits the solution

$$\begin{aligned} x(s) &= \left(\exp(-c) - \frac{b}{c}\right)\exp(-c(s-s_1)) + \frac{b}{c} \\ &\quad -b(s-s_1)\exp(-c(s-s_1)), \end{aligned} \tag{B.11}$$

where we have used (B.8) for x_1. At time $s = s_1 + 1$,

$$x(s_1+1) = \underline{x_2 \equiv \left(\exp(-c) - \frac{b}{c} - b\right)\exp(-c) + \frac{b}{c}}. \tag{B.12}$$

B.3. $s_1 + 1 \le s < P$

The last time interval that we need to consider is the interval $s_1 + 1 \le s < P$. Evaluating (B.11) at $s - 1$ leads to

$$\begin{aligned} x(s-1) &= \left(\exp(-c) - \frac{b}{c}\right)\exp(-c(s-s_1-1)) + \frac{b}{c} \\ &\quad -b(s-s_1-1)\exp(-c(s-s_1-1)). \end{aligned} \tag{B.13}$$

With (B.13), Eq (B.2) becomes

$$\begin{aligned} \frac{dx}{ds} &= b\left[\begin{array}{c} 1 - \left(\exp(-c) - \frac{b}{c}\right)\exp(-c(s-s_1-1)) - \frac{b}{c} \\ +b(s-s_1-1)\exp(-c(s-s_1-1)) \end{array}\right] - cx \\ x(s_1+1) &= x_2. \end{aligned} \tag{B.14}$$

The solution of Eq (B.14) is

$$\begin{aligned} x &= x_2\exp(-cu) + \frac{b}{c}(1-\frac{b}{c})(1-\exp(-cu)) \\ &\quad -bu\exp(-cu)(\exp(-c) - \frac{b}{c}) + \frac{b^2}{2}u^2\exp(-cu), \end{aligned} \tag{B.15}$$

where $u \equiv s - s_1 - 1$. Using (B.12), we eliminate x_2 in (B.15) and obtain

$$\begin{aligned} x &= \left[\exp(-2c) - (\frac{b}{c} + b)\exp(-c) + (\frac{b}{c})^2\right]\exp(-cu) \\ &\quad +\frac{b}{c}(1-\frac{b}{c}) \\ &\quad -\left[\exp(-c) - \frac{b}{c}\right]bu\exp(-cu) + \frac{b^2}{2}u^2\exp(-cu). \end{aligned} \tag{B.16}$$

B.4. $s = P$

At $s = P$, $x(P) = x_0$, and $u = u_P \equiv P - s_1 - 1$. From (B.16), we determine a first relation between x_0 and $u_P \equiv u(P)$:

$$\begin{aligned} x_0 &= \left[\exp(-2c) - (\frac{b}{c} + b)\exp(-c) + (\frac{b}{c})^2\right]\exp(-cu_P) \\ &\quad + \underline{\frac{b}{c}(1 - \frac{b}{c})} \\ &\quad - \left[\exp(-c) - \frac{b}{c}\right] bu_P \exp(-cu_P) + \frac{b^2}{2}u_P^2 \exp(-cu_P). \end{aligned} \tag{B.17}$$

A second condition is obtained by using (B.13) and requiring that $x(P-1) = 1$. We find

$$\left(\exp(-c) - \frac{b}{c}\right)\exp(-cu_P) + \frac{b}{c} - bu_P \exp(-cu_P) = 1. \tag{B.18}$$

The solution for cu_P as a function of b/c is given in implicit form by

$$\underline{\frac{b}{c} = \frac{1 - \exp(-c)\exp(-cu_P)}{1 - \exp(-cu_p) - cu_P \exp(-cu_P)}}. \tag{B.19}$$

With $c = 0.5$ fixed, we progressively increase cu_P from 0.1 to 0.8 and compute b using (B.19). At $b = 3.894$, $cu_P = 0.463$, implying $u_P = 0.992$. We determine x_0 from Eq (B.17). The latter can be simplified by using Eq (B.18). To this end, we formulate an expression for $1 - b/c$ from Eq (B.18). It is given by

$$1 - \frac{b}{c} = \left(\exp(-c) - \frac{b}{c}\right)\exp(-cu_P) - bu_P \exp(-cu_P). \tag{B.20}$$

Inserting (B.20) into Eq (B.17) (underlined term) and simplifying, we find

$$\underline{x_0 = \exp(-cu_P)\left[\begin{array}{c} \exp(-2c) - b\exp(-c) \\ -\exp(-c)bu_P + \frac{b^2}{2}u_P^2 \end{array}\right]}. \tag{B.21}$$

With $u_P \simeq 0.922$, we evaluate x_0 from Eq (B.21) and find $x_0 = 1.445$. It is in agreement with the numerical value of x_0 obtained from the numerical solution of the DDE.